 doi:10.20944/preprints202011.0272.v1

Article

Assessment of the impact of shot peening on the fatigue life of a compressor blade subjected to resonance vibrations

Arkadiusz Bednarz [1,*] and Wojciech Z. Misiolek [2]

[1] Department of Aircraft and Aircraft Engine, Rzeszow University of Technology; abednarz@prz.edu.pl
[2] Loewy Institute, Lehigh University, wzm2@lehigh.edu
* Correspondence: abednarz@prz.edu.pl; Tel.: +48 17 743 2348

Abstract: The publication presents the assessment of the influence of surface treatment such as shot-peening on the fatigue life of a compressor blade exposed to resonant vibrations. As part of the work, a geometric model of the blade was developed and a numerical modal and fatigue analysis were performed. The fatigue analysis was based on the Manson-Coffin-Basquin and Ramberg-Osgood models. As part of the work, the influence of different values of residual stresses on the results of fatigue life was determined. Additionally, the location of the highest equivalent stresses was established. The obtained results of the numerical analyzes were compared with the results presented in the scientific literature. An additional aim of the study was to determine the size of the grains at various points of the blade as well as the thickness of the layer plasticized as a result of peening. The obtained results are presented in the form of tables and charts. The relationship between the location of the highest values of equivalent stresses and the thickness of the plasticized layer was determined. The explanation of the effect of shot peening on the increase in fatigue life of the blade was proposed.

Keywords: fatigue life, crack initiation, resonance, shot peening, residual stress

1. Introduction

Compressor blades are often called the critical elements of the turbine aircraft engine. This statement is connected to the blade geometry, work conditions, and potential failures. Blades from are thin in the comparison to the rest of the geometrical parameters. This feature causes that the blade is susceptible to resonant bending. On the other hand, the aero dynamical and centrifugal forces as a result of high rotational velocity act on the examined blade [1-2]. The main function of the compressor is to create high pressure to allow energy transmitted by blades to be transformed into kinetic energy of the working fluid. In next components of the turbine engine, this air is mixed with fuel and burned. The generated fumes drive the turbine vanes and also create thrust of the engine.

The proper work of a compressor blade is important from many points of view. The quality and condition of the blade influences the compression process and hence the effectiveness of the engine. Theoretical damage could injure the blades (and vanes) next in engine assembly what could cause total damage of the engine. The aircraft history is full of cases of airplane accidents caused by destroyed compressor blades.

The working compressor vanes create a negative pressure for the air intake which could be responsible for sucking small elements from the surrounding such as small stones, grains of sand, even birds, etc. into the engine. The collision of the rotating blade with harder elements might create a notch on the blade surface [3-5]. If the notch is located close to the foot of the blade, usually it could be an origin of the future crack. The damaged blade used in service could cause crack propagation and it could break at the feather. Broken off the fragment of the blade may affect the balance of the compressor. Imbalance of the compressor can lead to resonance, which drastically decrease fatigue life of the whole engine.

 doi:10.20944/preprints202011.0272.v1

Working conditions and possible damage of the blades are included in the design and manufacturing process. In the production of aircraft engine blades, special alloys (super alloys) are used. In order to create blades more resistant to foreign object damage (FOD) and crack initiation [6], the feathers are usually subjected to shot-peening and special surfaces coatings are applied (e.g. to prevent corrosion).

Many papers dedicated to shot peening and its impact on the fatigue life are published in literature. Shot peening as a surface treatment has an astonishing impact on crack initiation and whole fatigue life of the treated element. The shot peening should be understood as a dynamic, plastic deformation surface treatment. The basis of this technology is to shot small balls on the treated surface to create plastic deformation and as a result a compressive stress on the surface of the treated element.

Depending on the process parameters it is possible to achieve residual stress with value – 1200 MPa [7]. The distribution and levels of the residual stress are dependent on kinetic energy and other parameters of the shot peening. The thickness of the plasticized layer may reach up to 100 μm (0.1 mm) [8]. Below this point, a quick increase in stress was observed reaching values close to zero [9]. Additionally, the microhardness may increase even to 500 HV [10]. For example, Zhang [8] observed an increase of hardness on the level equal to 60% (from 100 to value of 160 HV).

Chengfang [11] observed that, in the case of titanium alloy (super alloys) with residual stress equal to -750 MPa, the specimens achieve 67 times higher fatigue life. On the other hand, Daoxia [7], in case of residual stress equal to -1200 MPa, for steel, specimens achieve 4.5 time higher fatigue life. Gao [12] said that after shot peening up to the residual stress level of -350 MPa, the specimens achieved 5 fold increase in fatigue life. Maleki [13] showed that, in case of residual stress equal to -650 MPa, in the AISI 1045specimens observed 10 times higher fatigue life. Similar observations were made by Hammond [14], Seddik [15] and Dongxing [16]. Based on the above analysis, it was found that there is no simple relationship between the level of initial/residual stress and change in fatigue life.

Tekeli in his work [17] observed that in case of brittle steel (SAE 9245), increase of fatigue life was equal to 30% when residual stress was equal to -480 MPa and the depth of the plasticized layer was equal to 33 μm.

The main goal of the presented paper is to show the impact of the shot peening on the fatigue life of the compressor blade, under controlled geometry with notch created by machining, subjected to resonance vibrations. Obtained results are used to explain the influence of the depth of the plasticized material layer on crack initiation and its propagation. The obtained results are of great importance for the safety of air transport.

2. Numerical analysis

2.1. Analysis assumptions

As part of the numerical analysis, a geometric model of the blade was built and the fatigue model of the EI-961 material for the ε-N analysis was developed. The geometric model included a geometric notch (no pre-stress). The blade was subjected to modal analysis in order to determine the stress distribution in the area of the notch during resonance bending. The information obtained from the performed analysis was used to determine the fatigue life of the tested blade. The obtained results were compared with the results for the tested blade published in literature [3,5], made of from the same material – EI-961.

Preprints (www.preprints.org) | NOT PEER-REVIEWED | Posted: 9 November 2020 doi:10.20944/preprints202011.0272.v1

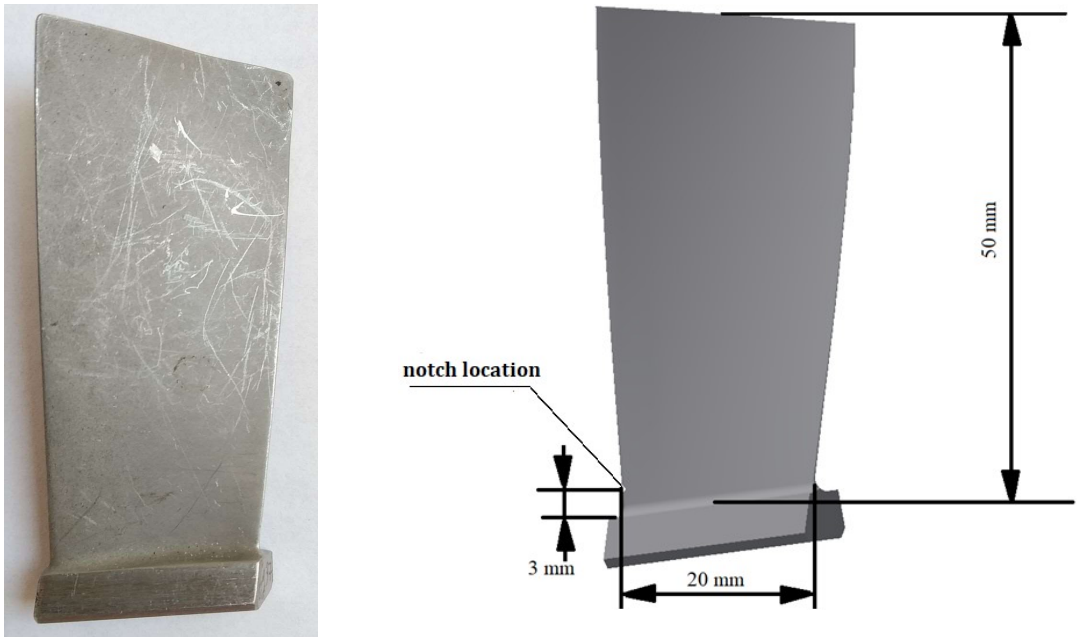

Figure 1. View of the examined blade **(a)** and geometrical model **(b)** used in numerical analysis.

The object of our studies was the first stage compressor blade of the PZL-10W turbine engine [3,4]. This blade (Fig. 1a) is made of the alloy EI-961 (0.1-0.16% C, 10.5-12.5% Cr, 0.35-0.5% Mo, 1.5-1.8% Ni, 0.18-0.3% V). It is an alloy with Young's modulus E = 200 GPa, density ρ = 7800 kg/m^3, tensile strength UTS = 1200 MPa, yield strength σ_Y = 1000 MPa and Poisson coefficient ϑ = 0.3. The aforementioned values are necessary to perform numerical modal analysis, as well as to estimate the fatigue constants for this alloy.

The performed fatigue analysis was based on the Manson-Coffin-Basquin equation (1), the result of which is the total strain amplitude, and the input data is the number of load cycles N and fatigue constants.

$$\frac{\Delta\varepsilon}{2} = \frac{\sigma_f'}{E}(2N)^b + \varepsilon_f'(2N)^c, \quad (1)$$

Within this model, it is necessary to estimate 4 material constants: σ_f' - fatigue strength coefficient, b - fatigue strength exponent, ε_f' - fatigue ductility coefficient, c - fatigue ductility exponent. These values were taken from literature [3] and were defined as the arithmetic mean value: σ_f' = 1651.94 MPa, b = -0.06, ε_f' = 0.33, c = -0.57.

Preprints (www.preprints.org) | NOT PEER-REVIEWED | Posted: 9 November 2020 doi:10.20944/preprints202011.0272.v1

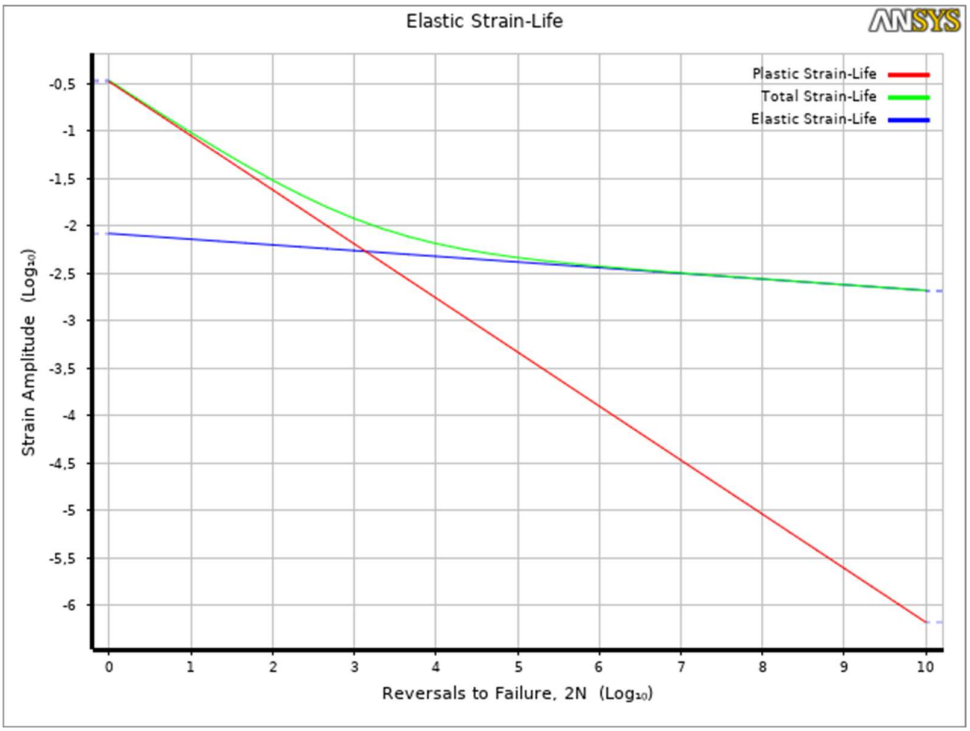

Figure 2. Strain-Life curve for EI-961 alloy (based on Manson-Coffin-Basquin equation).

Due to the fact that the modal analysis is based solely on the linear material model, and the EI-961 alloy is characterized by hardening, it is necessary to use the Ramberg-Osgood equation (2) to determine the total deformation (elastic and plastic components).

$$\Delta\varepsilon = \frac{\Delta\sigma}{E} + 2\left(\frac{\Delta\sigma}{2K\prime}\right)^{1/n\prime}, \quad (2)$$

To determine the strain amplitude (Δε), it is necessary to estimate two values: K'- cyclic strength coefficient and n' - cyclic strain hardening exponent. These values were determined based on data published in literature [3] and are respectively: K' = 2053.27 MPa and n' = 0.172.

The obtained data for the Manson-Coffin-Basquin equation and the Ramberg-Osgood equation were used to carry out the fatigue analysis based on the author's (AB) calculation program.

2.2. Subsection

Based on the real blade specimen dimensions, a geometric model was created. It includes a geometric notch (V-type) 0.5 mm deep and located 3 mm from the foot of the blade (Fig. 1b). The rounding radius at the bottom of the notch was 0.05 mm. In the bottom of the notch, its width of 1.02 mm was observed.

The geometric model of the notched blade was discretized with a finite element mesh with a dimension not exceeding 0.01 mm in the bottom of the notch. The discrete model consisted only of tetrahedral elements (TET-10) with square shape functions. The prepared model was subjected to numerical modal analysis. The research was conducted using commercial ANSYS 19.2 software. The resonance frequency of the tested blade was 791.2 Hz. Experimental studies [3,5] showed that the tested element has the frequency of the first form of resonance vibrations in the range from 756 to 830 Hz.

During the resonant vibrations (with the first mode of free vibration) pure bending was observed. In the case of the vibration amplitude of 1.8 mm - measured as the displacement of the blade top - the stress concentration was recorded in the area of the notch bottom (Fig. 3). In order to better visualize the results, a graph was prepared (Fig. 4) showing the value of the equivalent stresses

Preprints (www.preprints.org) | NOT PEER-REVIEWED | Posted: 9 November 2020 doi:10.20944/preprints202011.0272.v1

in the bottom of the notch, depending on the distance from the inner side of the blade, included in the relative values.

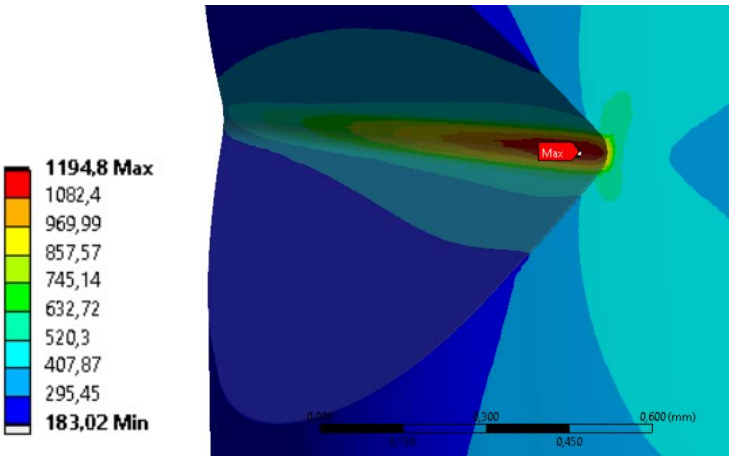

Figure 3. Equivalent stress σ_{EQV} (MPa) distribution in the bottom of the notch, in case of resonance vibration with an amplitude equal to 1.8 mm.

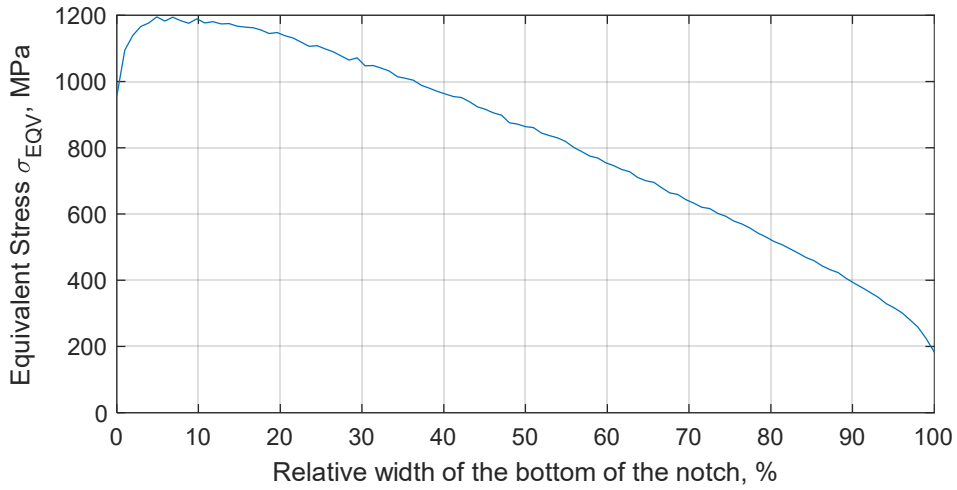

Figure 4. A plot of equivalent stress σ_{EQV} (MPa) in the bottom of the notch, in case of resonance vibration with an amplitude equal to 1.8 mm.

The observed equivalent stresses in the bottom are close to the value of the tensile strength (UTS) for this alloy. At the very edge of the element, the equivalent stresses reach a value slightly lower than the yield point (σ_Y) and amount to $\sigma_{EQV} = 955\,MPa$ (yield strength σ_Y = 1000 MPa).The maximum value of equivalent stresses $\sigma_{EQV} = 1194\,MPa$ is at the bottom of the notch, approximately 0.07 mm (70 μm) from the inner side of the blade. It concludes that the maximum value of stresses is not observed at the edge of the notch, but at its bottom. This in turn has a significant impact on fatigue life. Taking into account the fact of applied surface treatment (shot-peening), the initial/residual stress ratio from the blade surface (identical to the notch edge) will significantly increase the fatigue life. The stress component Z, related to the axis/height of the blade, has the greatest influence on the level of equivalent stress.

In the next step, the calculated values of equivalent stresses were used for fatigue analysis based on the previously mentioned Manson-Coffin-Basquin model. The performed ε-N analysis in the original assumes a pendulum load cycle. In subsequent iterations, different values of the residual

Preprints (www.preprints.org) | NOT PEER-REVIEWED | Posted: 9 November 2020 doi:10.20944/preprints202011.0272.v1

stresses were taken into account, from -100 to -500 MPa. Taking pre-stress values into account changes the load cycle to two-sided with a negative average value. The results of the conducted analyzes are summarized in Tables 1 and 2.

Table 1. Results of the numerical fatigue analysis based on the equivalent stress at the notched edge, with the amplitude of resonant vibrations of 1.8 mm.

	Assumed value of residual/initial stresses created by shot-peening					
	$0\ MPa$	$-100\ MPa$	$-200\ MPa$	$-300\ MPa$	$-400\ MPa$	$-500\ MPa$
Eqv. stress on the edge of the notch $\sigma_{EQV} = 955\ MPa$	117	405	$1.89 \cdot 10^3$	$17 \cdot 10^3$	$875 \cdot 10^3$	$259 \cdot 10^6$

In the first discussed case (when $\sigma_{EQV} = 955\ MPa$), assuming no residual stresses resulting from surface treatment, only 117 load cycles are needed to initiate a crack (Tab. 1). In the case of residual stresses of -200 MPa, the number of cycles to crack initiation increased 16 times. Further increase of residual stress to -300 MPa caused about 9 times increase in service life (to value $17 \cdot 10^3$).

In turn, in the case of fatigue analysis based on the maximum value of equivalent stresses ($\sigma_{EQV} = 1194\ MPa$), if the residual stresses are not taken into account, only 11 cycles are required to initiate a crack (Tab. 2). Only when the residual stresses of -500 MPa are taken into account, the observed durability is at the level of $6.39 \cdot 10^3$ load cycles.

Table 2. Results of the numerical fatigue analysis based on the maximum value of the equivalent stress, with the amplitude of resonance vibrations of 1.8 mm.

	Assumed value of residual/initial stresses created by shot-peening					
	$0\ MPa$	$-100\ MPa$	$-200\ MPa$	$-300\ MPa$	$-400\ MPa$	$-500\ MPa$
Max. value of eqv. stress $\sigma_{EQV} = 1194\ MPa$	11	28	76	243	987	$6.39 \cdot 10^3$

In experimental studies [3] it was proved that a crack with a length of 0.2 mm is observed after about $12.9 \cdot 10^3$ load cycles. Moreover, these tests show that the fracture starts right at the bottom of the notch, not at its edge. Due to the complex load condition in the bottom of the notch as well as on the blade surface (residual stresses presence), it would be difficult to accurately estimate the number of cycles to initiate such a crack size.

3. Metallography

The next step of the research was the performance of metallographic analysis, which resulted in information on the thickness of the layer exhibiting plastic deformation due to shot-peening, as well as the average grain size depending on the location within the blade (Figure 5).

Preprints (www.preprints.org) | NOT PEER-REVIEWED | Posted: 9 November 2020 doi:10.20944/preprints202011.0272.v1

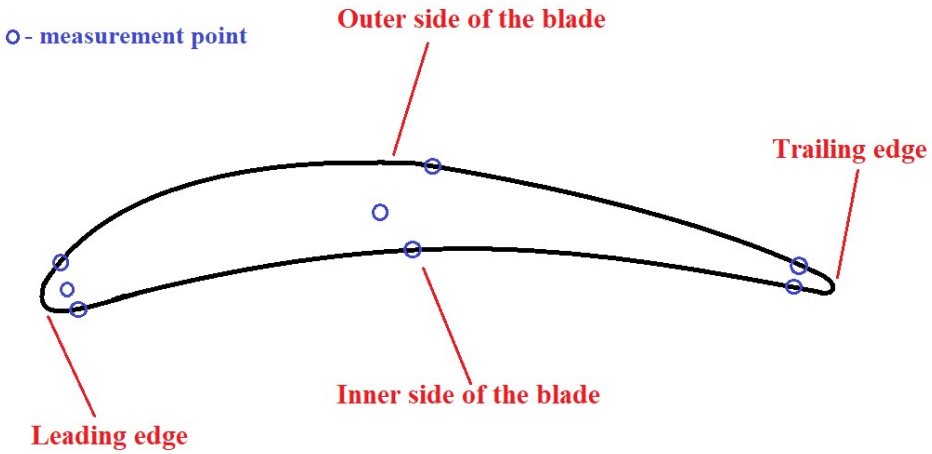

Figure 5. Measurement point locations and geometrical definitions of the sides of the blade.

The compressor blade (Figure 1a) was cut with a diamond saw into 8 mm thick samples. These samples were mounted using a resin and polished. In the last step, the samples were subjected to etching to emphasize the grain size and presence of grain boundaries (Figure 6). The marbles etchant (H2O, HCl, CuSo4) were used while electrolysis etching for 20 seconds each sample. The sample prepared in typical metallography techniques were observed under an optical microscope. Using the image analysis software, a series of photographs were taken showing the grain size at different points within the blade profile (Figure 6). The size of a single grain was measured, as well as the thickness of the layer plasticized as a result of surface treatment - shot-peening. The measurement was made on both sides of the blade profile, at six characteristic points (at the leading edge, in the middle part, and at the trailing edge - on the inner and outer side of the profile), as well as at two points inside the profile. The locations of the points are presented in Figure 5. It should be remembered that the inner side of the blade is the working side that is most exposed to erosive action and that the leading edge is most exposed to collision with hard elements sucked into the engine. The obtained grain measurement results are presented in Figures from 8 to 10.

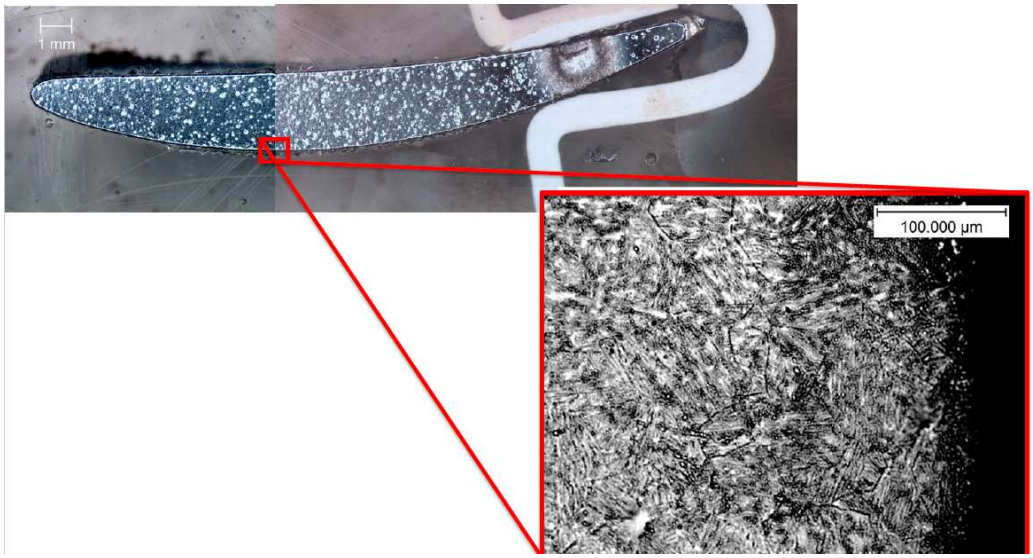

Figure 6. Picture of the cross-section with a magnified grain image from the center outer side of the blade.

Preprints (www.preprints.org) | NOT PEER-REVIEWED | Posted: 9 November 2020 doi:10.20944/preprints202011.0272.v1

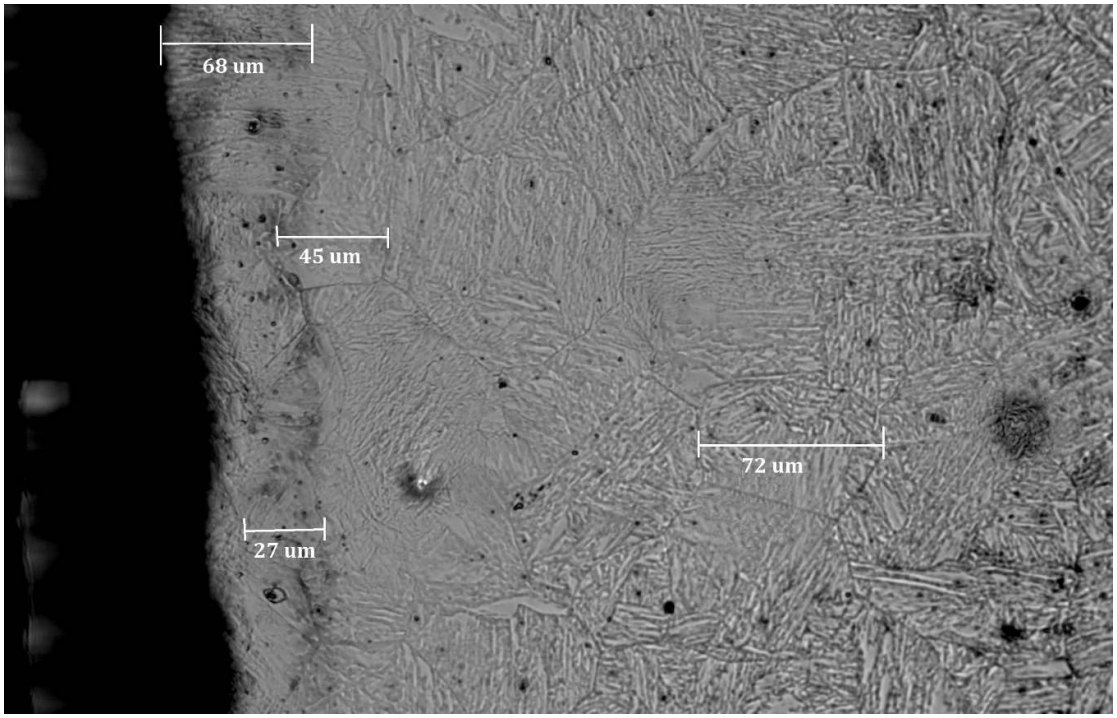

Figure 7. View of the microstructure within the 7th cross-section, on the inner side of the blade with marked representative dimensions (grain size and depth of the plasticized layer).

As shown in Figure 7, it was possible to measure the size of the grains and the thickness of the plasticized layer using standard metallography techniques. A distinctive boundary between the plasticized zone and the non-plasticized zone is present. The representative grain size of the native material is 72 μm, while at the edge the grain size is about 27 μm. The thickness of the plasticized layer in this part of the blade was 68 μm. In the presented cross-section, the smaller thickness of the plasticized zone by peening is observed.

As a result of the performed work, the smallest grains were observed on the inner side of the blade (Figure 8), at the leading edge (26 μm), while the largest at the trailing edge of the profile - 47 μm). This tendency continues until about half the height of the blade. At the tip of the blade, the largest grains are observed in the middle (48 μm) of the inner side of the blade. In the case of the outer side, the smallest grains are observed near the leading edge (27 μm), and the largest (up to 3 times larger) in the middle part of the profile (46 μm). In the case of the native material (inner side of the blade), there is a tendency that in the part at the leading edge, the grains are almost 2 times larger than in the central part. Generally, the grains are 25 to 72 μm on the inner side and 23 to 76 μm on the outer side. In the case of the native material in the leading edge zone, the grains range in size from 102 μm (at the root) to 39 μm at the tip of the blade.

The distance from the root of the blade also affects the thickness of the plasticized layer (Figure 9). For the leading edge zone, on both the inside and outside of the blade, a layer thickness of more than 150 μm was observed. For the central part of the blade as well as the outer side, the plasticized layer exceeds 100 μm but does not exceed 150 μm. The greater the distance from the foot of the blade, the thickness of the plasticized layer at the leading edge significantly decreases. At the tip of the blade, the smallest thickness of this layer was recorded for the leading edge. The layer thickness in the trailing edge part is not much greater.

Preprints (www.preprints.org) | NOT PEER-REVIEWED | Posted: 9 November 2020 doi:10.20944/preprints202011.0272.v1

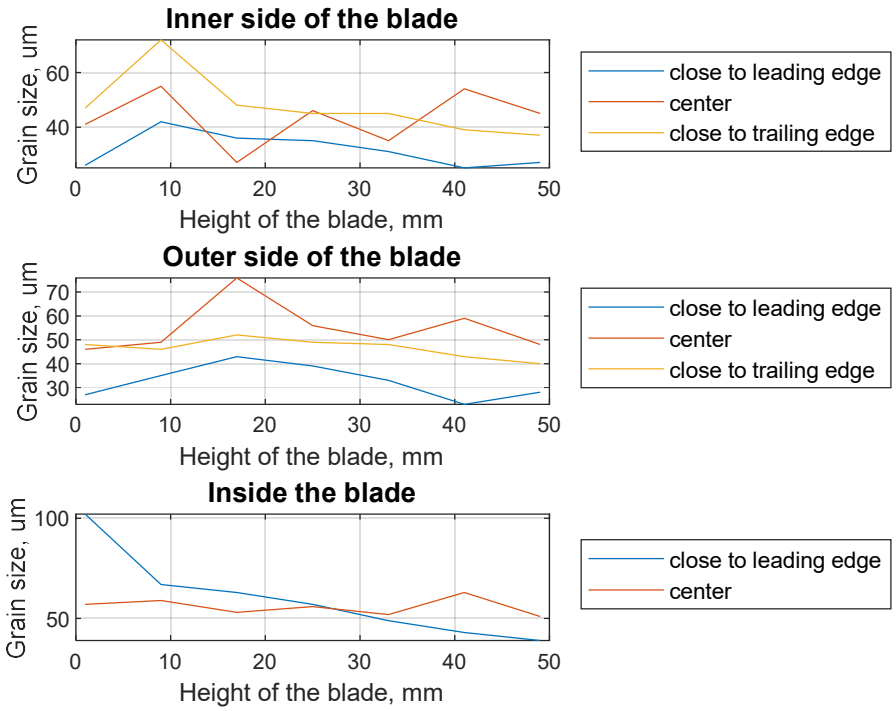

Figure 8. Plots of grain size (in the layer plasticized by shot-peening) in the function of the height of the blade for different location of measurement.

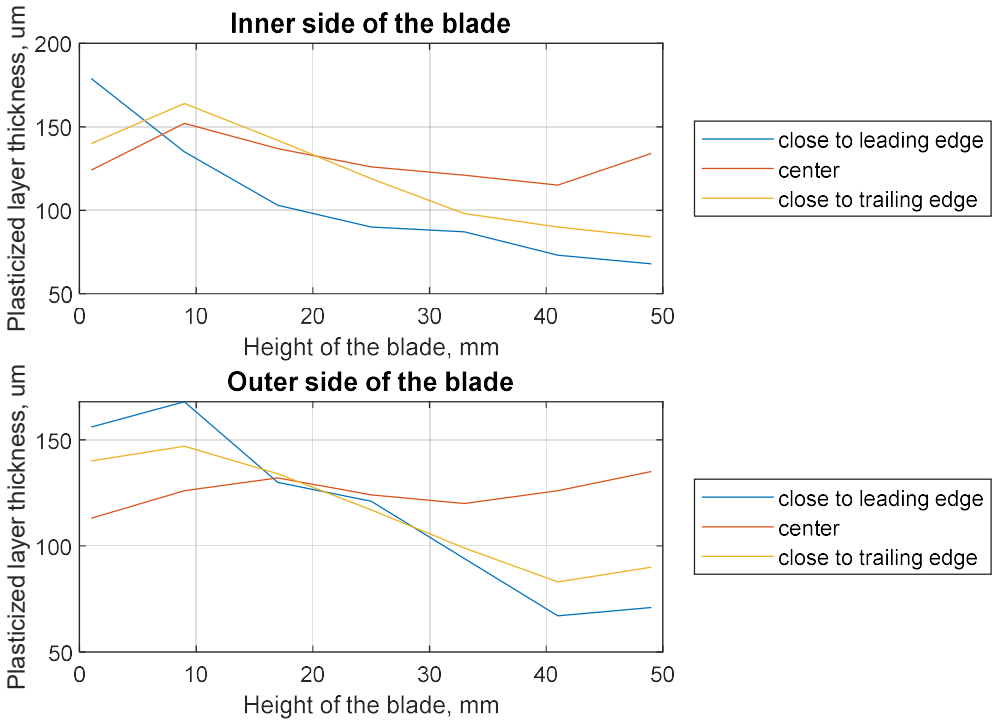

Figure 9. Plots of plasticized layer thickness (by shot-peening) in the function of the height of the blade for different location of measurement.

Preprints (www.preprints.org) | NOT PEER-REVIEWED | Posted: 9 November 2020 doi:10.20944/preprints202011.0272.v1

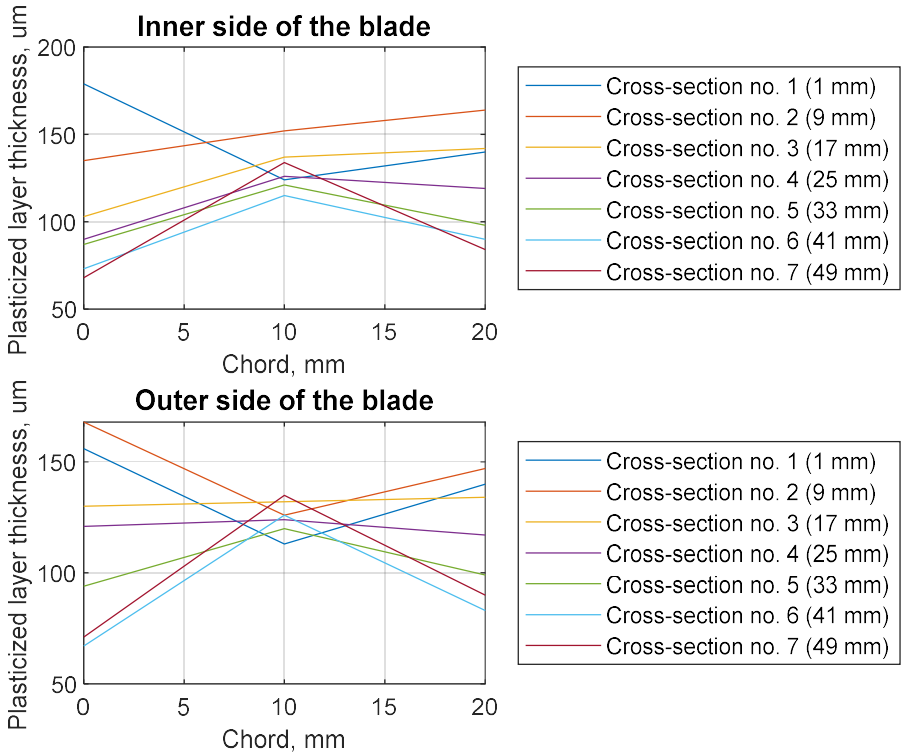

Figure 10. Plots of plasticized layer thickness (by shot-peening) in the function of the chord of the blade for a different side of the blade, for different cross-sections.

The change in the thickness of the plasticized layer was also verified depending on the chord of the blade and the tested cross-section (Figure 10). In parentheses, there is information about the distance between the foot of the blade and the given parallel cross-section. Both on the inside and outside of the blade, in the central part of the blade, the smallest scatter in the obtained results was observed. In the case of the edges, the trends described in the discussion of Figure 9 are observed. In the case of cross-sections 1 and 2 (on the outer side of the blade), it was observed that the edges of the blade had a greater thickness of the plasticized layer. This tendency is not observed in the remaining cross-sections.

The tested blade has not been used before testing and analysis, and the observed fatigue life corresponds to approximately 216 minutes of operation in the resonance state. Taking into account the fact that, the duration of a typical flight exceeds 3 hours, there is a risk of an early rupture of the blade in the event of damage and a simultaneous resonance state. The location of the notch also affects (increases?) the possibility of blade breaking. The further away from the root of the blade, the notch is located the less chance of the blade breaking and lower possibility of serious damage of the jet engine and the aircraft. This possibility is associated with both the reduction of stresses in the resonant state, as well as a small decrease in the thickness of the deformed zone of the blade due to applied surface treatment.

4. Conclusions

The obtained results of the numerical fatigue analysis show that during the vibration of the compressor blade with a geometric notch, stresses occurring close to the tensile strength for a given alloy. The classic approach related to the determination of the fatigue life by the Manson-Coffin-Basquin model does not give satisfactory results. Only taking into account the values of initial/residual stresses resulting from surface treatment allows us to obtain more accurate results. Experimental studies related to the determination of the thickness of the plasticized layer show that

the area of maximum reduced stress values is contained in this zone. Thanks to this approach, it is possible to increase the durability of the blade.

Future research should focus on the accurate determination of the initial stress values on the blade surface as well as the optimized fatigue data determination method for numerical fatigue analysis.

Acknowledgement: This research was funded by the Department of Aircrafts and Aircraft Engines, Rzeszow University of Technology (DS.ML.20.001) and by the Fulbright Program (sponsored by the U.S. Department of State).

References

1. Dixon, S.L.; Hall, C.A. Fluid Mechanics, and Thermodynamics of Turbomachinery, 7th ed.; Butterworth-Heinemann: Oxford, Great Britain, 2014.
2. Shun-Peng, Z.; Peng, Y.; Zheng-Yong, Y.; Qingyuan, W. A Combined High and Low Cycle Fatigue Model for Life Prediction of Turbine Blades. *Materials* **2017**, *10 (7), 698*, pp. 1–15.
3. Bednarz, A. Evaluation of Material Data to the Numerical Strain-Life Analysis of the Compressor Blade Subjected to Resonance Vibrations. *Advances in Science and Technology Research Journal* **2020**, *14(1),* pp. 184–190.
4. Bednarz, A. Influence of the Amplitude of Resonance Vibrations on Fatigue Life of a Compressor Blade with Simulated FOD Damage. *Advances in Science and Technology Research Journal* **2020**, *14(3),* pp. 22–29.
5. Witek, L.; Bednarz, A.; Stachowicz, F. Fatigue analysis of compressor blade with simulated foreign object damage. *Engineering Failure Analysis* **2015**, *58*, pp. 229-237.
6. Zahavi, E.; Torbilo. V. Life expectancy of machine parts: Fatigue Design. CRC Press Inc: Boca Raton, USA, 2011; pp. 101-140 and 239-258.
7. Daoxia, W.; Changfeng, Y.; Dinghua, Z. Surface characterization and fatigue evaluation in GH4169 superalloy: Comparing results after finish turning; shot peening and surface polishing treatments. *International Journal of Fatigue* **2018**, *113*, pp. 222–235.
8. Zhang, P.; Lindemann, J. Influence of shot peening on high cycle fatigue properties of the high-strength wrought magnesium alloy AZ80. *Scripta Materialia* **2005**, *52*, pp. 485–490.
9. Qiong, W.; Dong, X.; Zhemin, J.; Yidu, Z.; Huazhao, Z. Effect of shot peening on surface residual stress distribution of SiCp/2024Al. *Composites* **2018**, *154,* pp. 382–387.
10. Klotz, T.; Delbergue, D.; Bocher, P.; Lévesque, M.; Brochu, M. Surface characteristics and fatigue behavior of shot peened Inconel 718. *International Journal of Fatigue* **2018**, *110*, pp. 10–21.
11. Changfeng, Y.; Daoxia, W.; Lufei, M.; Liang, T.; Zheng, Z.; Jiyin, Z. Surface integrity evolution, and fatigue evaluation after milling mode, shot-peening and polishing mode for TB6 titanium alloy. *Applied Surface Science* **2016**, *387*, pp. 1257–1264.
12. Gao, Y.K. Improvement of fatigue property in 7050–T7451 aluminum alloy by laser peening and shot peening. *Materials Science and Engineering* **2011**, *528*, pp. 3823–3828.
13. Maleki, E.; Unal, O.; Kashyzadeh, K.R. Fatigue behavior prediction, and analysis of shot-peened mild carbon steels. *International Journal of Fatigue* **2018**, *116*, pp. 48–67.
14. Hammond, D.W.; Meguid, S.A. Crack propagation in the presence of shot-peening residual stresses. *Engineering Fracture Mechanics* ***1990***, *37(2),* pp. 373-387.
15. Seddik, R.; Sghaier, R.B.; Atig, A.; Fathallah, R. Fatigue reliability prediction of metallic shot peened-parts based on Wöhler curve. *Journal of Constructional Steel Research* **2017**, *130,* pp. 222–233.
16. Dongxing, D.; Daoxin, L.; Xiaohua, Z.; Jingang, T.; B, M. Effects of WC-17Co Coating Combined with Shot Peening Treatment on Fatigue Behaviors of TC21 Titanium Alloy. *Materials* **2016**, *9(11)*, 865.
17. Tekeli, S. Enhancement of fatigue strength of SAE 9245 steel by shot peening. *Materials Letters* **2002**, *57*, pp. 604–608.